

钛合金表面氩弧熔覆 TiC 增强复合涂层组织与性能分析

王振廷^{1,2}, 陈丽丽², 张显友¹

(1. 哈尔滨理工大学 材料科学与工程博士后流动站, 哈尔滨 150080;

2. 黑龙江科技学院 材料科学与工程学院, 哈尔滨 150027)

摘 要: 把石墨粉末预涂在钛合金表面上, 利用氩弧熔覆技术成功制备出原位自生 TiC 增强的金属基复合涂层。利用扫描电镜、X 射线衍射仪和能谱仪分析了熔覆涂层的显微组织, 探讨了增强相 TiC 的生成机制; 利用显微硬度仪测试了复合涂层的显微硬度并用磨损试验机考察了其在室温干滑动磨损条件下的耐磨性能。结果表明, 氩弧熔覆涂层组织均匀致密, 原位自生 TiC 呈树枝晶和细碎的条状均匀地分布于整个涂层中; 由 TiC 增强的复合涂层明显地改善了钛合金的表面硬度, 平均硬度约为 700 HV0.2 且沿层深方向呈梯度分布; 涂层在室温干滑动磨损条件下的耐磨性明显优于基体, 约为钛合金的 10.5 倍。

关键词: 钛合金; 氩弧熔覆; 原位自生; 涂层; 显微组织

中图分类号: TG174 **文献标识码:** A **文章编号:** 0253-360X(2008)09-0043-03



王振廷

0 序 言

钛合金具有优异的综合性能, 如良好的耐蚀性、高比强度以及良好的生物相容性, 在航空航天、石油化工和生物医学等领域具有广阔的应用前景。但钛合金摩擦系数大、耐磨性差使其工业应用受到了很大限制。近年来, 采用离子注入、热氧化、粒子束增强沉积、化学镀、激光表面合金化、激光表面熔覆 PVD、CVD 等表面改性技术已经使得钛合金的表面性能得到了明显的改善^[1]。而利用原位反应合成高硬度陶瓷材料 TiC、TiB₂、TiN 等增强的金属基复合涂层, 由于增强相具有热力学稳定、尺寸细小、分布均匀、界面洁净、与基体结合良好的特点, 从而提高界面强度, 已经成为近几年研究的热点。

在众多的陶瓷材料增强体中, TiC 由于具有较高的硬度和熔点以及较好的热稳定性, 在复合材料中对金属基体的韧度损害较小, 所以在制备耐磨复合材料领域得到了广泛应用^[2]。目前原位合成 TiC 颗粒增强金属基复合涂层的方法主要有激光熔覆、感应熔覆和等离子熔覆^[3-7]。然而, 利用具有投资和运行费用低、操作灵活等优点的氩弧熔覆方法制

备 TiC 增强复合涂层方法的研究相对较少。为此, 采用氩弧熔覆技术, 在钛合金表面原位合成了 TiC 陶瓷增强的金属基复合涂层, 并对涂层的组织和性能进行了研究。

1 试验方法

基体材料选工程用的镍钛合金。将其机械加工成尺寸为 30 mm×15 mm×10 mm 的试样。表面用砂轮打磨出金属光泽并用无水乙醇和丙酮清洗。预涂材料为石墨粉, 粉末的平均粒度为 30 μm, 纯度大于 99%。将石墨粉与粘结剂均匀地混合成膏状, 手工涂抹在试样表面, 厚度控制在 1.00 mm 左右, 并不断压实。自然阴干 24 h 后将试样放置在真空干燥箱中 150 °C 下烘干 2 h。用型号为 MW3000 的钨极氩弧焊机进行氩弧熔覆试验, 工艺参数为工作电压 14 V, 焊接电流 120 A, 氩气流量 12 L/min, 熔覆速度 4 mm/s。

采用电火花线切割(NH7720)沿垂直于熔覆层方向加工出横截面试样, 并用体积比为 2:1:10 的 HNO₃-HF-H₂O 混合溶液化学腐蚀; 采用 XJ-17A 型金相显微镜和 MX2600 扫描电镜进行组织观察; 并用 XD-2 型 X 射线衍射仪结合能谱分析仪(OXFORD)对熔覆层进行物相鉴定; 用 MHV2000 型显微硬度计测量涂层的硬度(载荷 1.96 N, 保持时间

10 s)。在 MM-200 摩擦磨损试验机上测试涂层的摩擦磨损性能,对磨偶件采用经淬火态的 GGr15 钢环,法向载荷 98 N,试验磨损时间为 60 min。试验前后用丙酮将试样清洗干净,烘干后用精度为 0.1 mg 的 SartoriusBS110 电子天平称量试样的磨损质量损失并以此作为衡量耐磨性的指标。

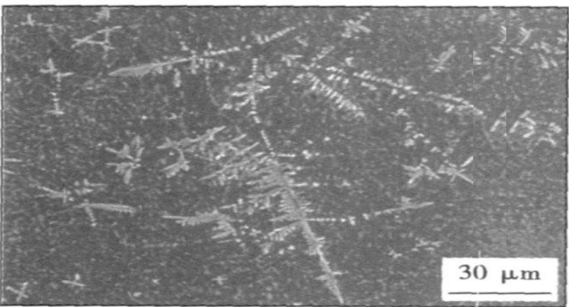
2 试验结果与分析

2.1 氩弧熔覆复合涂层显微组织

图 1 是钛合金表面氩弧熔覆 TiC 增强复合涂层组织形貌。从中可看出,熔覆层内部组织均匀,在黑色基体上弥散分布着生长良好的树枝晶和细碎的白色条状物。EDS 分析结果(质量分数, %):树枝晶 C 17.45, Ti 53.45;细碎的条状相 C 15.68 Ti 41.48;基体 C 10.26 Ti 39.69;其余为 Ni;结合 XRD (图 2)可以确定钛合金表面上预涂石墨粉经氩弧熔覆作用后,制得了以呈树枝晶和条状分布的 TiC 为增强相、TiNi 为基体的快速凝固复合涂层。衍射图中 TiC 峰的出现证明了在氩弧熔覆过程中 TiC 增强相可以由石墨和钛合金中的 Ti 元素原位反应合成。



(a) 复合涂层高倍组织形貌



(b) 复合涂层低倍组织形貌

图 1 氩弧熔覆复合涂层 SEM 形貌

Fig. 1 SEM micrographs of composite coating by GTAW

2.2 氩弧熔覆复合涂层的硬度及耐磨性

图 3 给出了熔覆试样从熔覆层表面到基体区的显微硬度分布图。可以看出熔覆层的显微硬度较基

体有了很大幅度的提高,平均硬度为 700 HV0.2。且沿着层深方向呈梯度渐降的趋势,但最低值仍然高于基体钛合金。文献[8]表明:Ti 是正偏析元素,常偏聚于最终凝固的区域。由于凝固界面是由熔池底部向自由表面推进,因此越接近熔池的自由表面,合金熔体中 TiC 形成元素的含量就越高,故熔覆层中的 TiC 多集中于熔池的上部。相应的,显微硬度分布也是由熔池底部向表面增加。

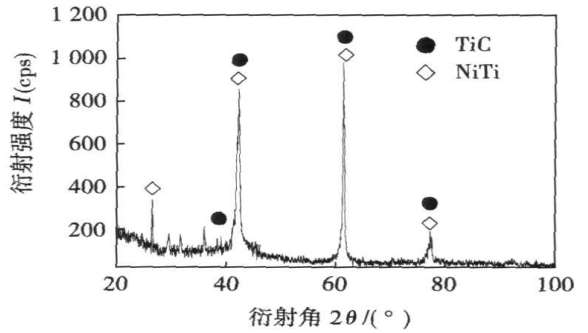


图 2 氩弧熔覆复合涂层 X 射线衍射图谱

Fig. 2 XRD pattern of composite coating by GTAW

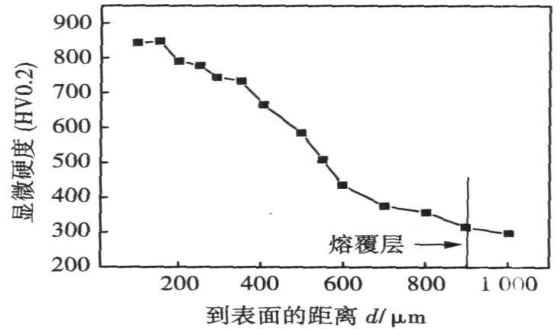


图 3 复合涂层的显微硬度分布曲线

Fig. 3 Microhardness profile of the composite coating

图 4 为复合涂层与基体在相同条件下的磨损失重—时间曲线,可以看出随着时间的延长复合涂层的磨损失重趋于稳定,而基体钛合金失重严重。

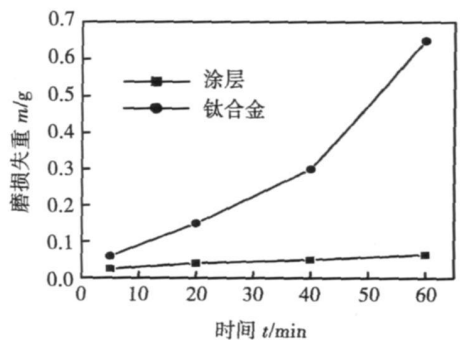


图 4 复合涂层与基体磨损失重—时间曲线

Fig. 4 Wear loss-time curves of composite coating and Ti alloy

从图5复合涂层与基体相对耐磨性可明显看出复合涂层的耐磨性得到了大幅度的提高,约为基体的10.5倍。

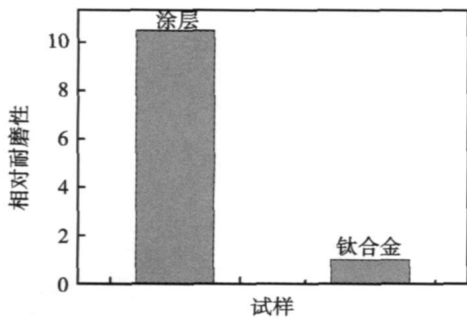


图5 涂层与基体相对耐磨性

Fig. 5 Wear resistance comparison between Ti alloy and coating

2.3 氩弧熔覆复合涂层中TiC形核与长大分析

对于反应 $Ti + C \rightarrow TiC$,

$$\Delta G^0 = -186\,606 + 13.2T \text{ (J/mol)}$$

当 $T < 14\,136\text{ K}$ 时, Ti 与 C 之间的反应生成 TiC 的 Gibbs 自由能 $\Delta G^0 < 0$, 钨极电弧温度满足此反应条件; 且按照热力学计算当 $T > 1\,373\text{ K}$ 时冶金反应 $Ti + C \rightarrow TiC$ 能够进行^[9], 而钨极氩弧熔覆方法中熔池的温度远高于这个温度, 因此, 在热力学上采用氩弧熔覆工艺完全有可能原位形成 TiC 颗粒。当用氩弧熔覆方法进行表面合金化的过程中, 高电流的作用使得钨极氩弧的热量迅速加热预涂粉末至熔化状态形成熔池, 合金元素发生相互扩散及各种物理、化学反应。

2.3.1 枝晶状 TiC 的形成

在熔池形成后的液相期内, Ti 和 C 原子反应生成稳定的 TiC 晶核。随着反应的进行, TiC 晶核形成数量不断增多, 熔池中的 Ti 和 C 含量不断降低, 当 Ti, C 原子浓度降至反应所需临界浓度以下时, 新反应生成的 TiC 不能以稳定晶核的形式存在, 只能在已生成的晶核上按照 TiC 晶体的优先生长方向堆积、长大, 形成 TiC 的发达树枝状分布形貌。并且观察到其生长表面有明显的棱面或小平面特征。

2.3.2 细碎的条状 TiC 的形成

由于氩弧熔覆表面合金化过程是一种快速熔化、快速凝固的非平衡过程, 电弧扫过后熔池迅速冷却至液相温度以下, 已经降至液相温度以下凝固的基体把形核后来不及长大的 TiC 包围, 形成了固态包

覆层, 因此, 在固态包覆层中的 Ti, C 原子只能通过原子扩散和渗透方式堆积到 TiC 晶核上并发生反应, 形成了尺寸较小的细碎的条状共晶 TiC, 在整个涂层中弥散分布。

3 结 论

(1) 以石墨粉末为原料, 采用氩弧熔覆方法在钛合金表面成功制备了 TiC 增强复合涂层。增强相 TiC 呈树枝晶状和细碎的条状分布在 NiTi 基体上, 组织均匀致密。

(2) 复合涂层的显微硬度有了很大提高, 平均硬度为 700 HV0.2; 在室温干滑动磨损条件下具有优异的耐磨性, 约为基体的 10.5 倍。

参考文献:

- [1] 王 影, 张凌云, 于茉莉, 等. 钛合金表面激光熔敷 $Ti_2Ni_3Si/NiTi$ 耐磨涂层组织与耐磨性能[J]. 稀有金属材料与工程, 2006, 35(1): 62-65.
- [2] 宋思利, 邹增大, 王新洪, 等. 多层氩弧熔敷含 TiC 颗粒增强涂层的微观组织及耐磨性能[J]. 焊接学报, 2007, 28(4): 33-37.
- [3] 邹东利, 阎殿然, 何继宁. 反应等离子喷涂 TiN 复相陶瓷涂层的研究[J]. 稀有金属材料与工程, 2007, 36(3): 225-229.
- [4] 朱警雷, 黄继华, 王海涛, 等. 反应等离子喷涂 TiC/Fe-Ni 金属陶瓷复合涂层的显微组织[J]. 中国有色金属学报, 2008, 18(1): 36-41.
- [5] 王振廷, 陈华辉. 感应熔敷纳米复合材料涂层组织及抗磨性能[J]. 粉末冶金技术, 2006, 24(1): 32-35.
- [6] 王振廷, 孟君晟, 王永东, 等. 原位自生 TiCp/Ni60A 复合涂层组织结构及长大特性[J]. 稀有金属材料与工程, 2007, 36(2): 709-711.
- [7] 于翔天, 王华明. 激光熔化沉积 (TiB+TiC)/TA15 显微组织[J]. 宇航材料工艺, 2007, 6: 106-110.
- [8] 陈 瑶, 王华明. TiAl 金属间化合物合金碳元素脉冲激光表面合金化显微组织及 TiC 快速凝固生长形态研究[J]. 应用激光, 2002, 22(2): 83-85.
- [9] 严有为, 魏伯康, 林汉同等. 化学成分对 TiCp/Fe 复合材料组织和性能的影响[J]. 中国有色金属学报, 1999, 9(2): 225-230.

作者简介: 王振廷, 男, 1965 年出生, 博士后, 教授, 硕士生导师。主要从事耐磨材料和材料表面工程方面的科研和教学工作。已发表论文 30 余篇。

Email: wangztl2002@163.Com

niversity of Aeronautics and Astronautics Nanjing 210016, China; 2. The 14th Research Institute, China Electronics Technology Group Corporation, Nanjing 210013, China). p35–38

Abstract Soldering experiments of fine pitch devices were carried out using diode-laser soldering system and IR reflow soldering with SnPb, SnAgCu, SnAg, and the tensile strengths of soldered joints were measured by Micro-joints Tester. The results indicate that mechanical properties of fine pitch devices soldered joints with laser soldering system is better than that of fine pitch devices soldered joints with IR reflow soldering method, especially for SnAg soldered joints, and the mechanical properties of lead-free soldered joints is also better than that of Sn-Pb solder. The characteristics of fracture morphology of micro-joints were also analyzed by SEM. It is found that the fracture mechanism of micro-joints soldered with laser soldering system is toughness fracture, and mangled edges appear in a fixed direction. While the fracture morphology of micro-joints soldered with IR reflow soldering method has less and lower dimples than that with diode-laser soldering system. Both the dimple crack mechanisms under the two soldering methods belong to transgranular crack.

Key words: diode-laser reflow; IR reflow; mechanical properties; fracture morphology

Effect of geometrical parameters of coil on electromagnetic force in coil-sheet system

XU Wei, LIU Xuesong, YANG Jianguo, FANG Hongyuan (State Key Laboratory of Advanced Welding Production Technology, Harbin Institute of Technology, Harbin 150001, China). p39–42, 54

Abstract: Based on the new idea of controlling welding stress with trailing electromagnetic force, the electromagnetic force in flat spiral coil-aluminum sheet system was simulated with finite element software ANSYS. Effect of geometrical parameters of coil on electromagnetic force was analyzed. The results show that the electromagnetic force acts on the location where the coil projects on the sheet. With decreasing outer diameter of the coil, the electromagnetic force peak magnitude increases and the peak position of the axial force moves linearly close to the inner side of coil. With increasing inner diameter, the radial force peak magnitude increases, the axial force peak magnitude increases first and then decreases, and the peak position of the axial force is fixed first and then moves close to outer side of coil. With increasing wire width, the electromagnetic force magnitude increases. The variation of the position, where the direction of the radial force is turned, with the inner and outer radius is similar to that of the peak position of the axial force. While controlling welding stress based on electromagnetic force, the coil with the smaller outer radius and the appropriate inner radius should be selected, and the magnetic medium is needed to enhance electromagnetic force.

Key words: electromagnetic force; geometrical parameters; flat spiral coil; welding stress

Microstructure and properties of TiC reinforced composite coating fabricated on Ti alloy by GTAW

WANG Zhenting^{1,2}, CHEN Lili², ZHANG Xianyou¹ (1. Mobile Postdoctoral Center of Materials Science and Engineering, Harbin University of Science and

Technology, Harbin 150080; 2. College of Materials Science and Engineering, Heilongjiang Institute of Science and Technology, Harbin 150027, China). p43–45

Abstract A metal matrix composite coating reinforced by TiC particulates has been successfully fabricated utilizing the in-situ reaction of pre-placed C powder on Ti alloy by gas tungsten arc welding (GTAW) process. The microstructure of the coating was analyzed by scanning electron microscopy (SEM), X-ray diffraction (XRD) and energy-dispersive spectrum (EDS). The growing mechanism of TiC was discussed. Microhardness and wear resistance at room temperature of the composite coating were examined by means of Microhardness Tester and Wear Tester respectively. The results show that microstructure of the composite coating is uniform and the fine TiC exhibits dendrite and strip shapes. The composite coating reinforced by in-situ TiC apparently improves surface hardness of Ti alloy, the average microhardness can reach HV700, and its gradient distribution appears. Wear resistance of the composite coating is about 10.5 times of Ti alloy's substrate.

Key words: Ti alloy; GTAW; in-situ synthesis; coating; microstructure

Residual stress field in hole-drilling method—part I: Theoretical analysis

LI Hao, LIU Yihua (School of Civil and Hydraulic Engineering, Hefei University of Technology, Hefei 230009, China). p46–50

Abstract During the residual stress measurement by using the hole-drilling method, a work-hardening layer near the hole will be formed due to the cutting force. As the material characteristics in the work-hardening layer will vary evidently, the layer surrounding the hole can affect the stress relieved after hole drilling. The work-hardening layer was simplified as a heterogeneous annulus by increasing the elastic modulus of the material near the hole, and the analytical solution of the release stresses after drilling in a infinite plate submitted to the biaxial uniform stresses was developed by using the method of elasticity. The release stresses in a 304 stainless steel plate under the biaxial stresses were numerically calculated by the FEM program MSC/Patran & Nastran and compared with the analytical solution. The results indicate that the simplified model is feasible and the analytical solution is valid. When the residual stresses are determined by using the hole-drilling method, it will be more accurate if the work-hardening layer is considered.

Key words: residual stress; hole-drilling method; work-hardening; modulus of elasticity; analytical solution

Abradability of Cu-Al₂O₃ gradient coatings by plasma spraying

LI Gaozhong^{1,2}, FENG Lajun¹, LEI A-li¹, XU Dapeng¹ (1. School of Materials Science and Engineering, Xi'an University of Technology, Xi'an 710048, China; 2. School of Materials and Chemical Engineering, Xi'an Technological University, Xi'an 710032, China). p51–54

Abstract Cu-Al₂O₃ gradient coatings were prepared by plasma spray. The microstructure and abraded superficial shape of the coatings were analyzed by metallography and SEM. The wear-resisting property of Cu-Al₂O₃ gradient ceramic coatings was tested by self-produce immobile wearing machine. The results show that the